Fish and Shellfish Immunology 95 (2019) 411–421

Contents lists available at ScienceDirect

Fish and Shellfish Immunology

journal homepage: www.elsevier.com/locate/fsi

Full length article

Glutaredoxin 2 from big belly seahorse (*Hippocampus abdominalis*) and its potential involvement in cellular redox homeostasis and host immune responses

W.K.M. Omeka[a,b], D.S. Liyanage[a,b], Hyerim Yang[a], Jehee Lee[a,b,*]

[a] Department of Marine Life Sciences & Fish Vaccine Research Center, Jeju National University, Jeju Self-Governing Province, 63243, Republic of Korea
[b] Marine Science Institute, Jeju National University, Jeju Self-Governing Province, 63333, Republic of Korea

ARTICLE INFO

Keywords:
Glutaredoxin
Redox homeostasis
Immune responses
Seahorse

ABSTRACT

Glutaredoxins are oxidoreductases present in almost all living organisms. They belong to the thioredoxin superfamily and share the thioredoxin structure and catalytic motif. Glutaredoxin 2 has been identified as a mitochondrial protein in vertebrates. In this study, the sequence of Glutaredoxin 2 from *Hippocampus abdominalis* (HaGrx2) was analyzed by molecular, transcriptional, and functional assays. *In-silico* analysis revealed that HaGrx2 shows the highest homology with *Hippocampus comes,* while distinctly cluster with fish Grx2 orthologs. Tissue distribution analysis showed that *HaGrx2* is ubiquitously expressed in all tissues tested, and the highest expression was observed in the brain and skin. Significant *HaGrx2* transcript modulation was identified in blood and liver upon injecting bacterial and Pathogen Associated Molecular Patterns. The redox activity of HaGrx2 was revealed by Dehydroascorbic reduction and insulin disulfide reduction activity assays. Further, the deglutathionylation activity of 1 nM HaGrx2 was found to be equivalent to that of 0.84 nM HaGrx1. HaGrx2 exhibited antiapoptotic activity against H_2O_2-induced oxidative stress in FHM cells. Altogether, the results of this study suggest that HaGrx2 plays a role in redox homeostasis and innate immune responses in fish.

1. Introduction

Glutaredoxins (Grxs) are glutathione-dependent oxidoreductases that are mainly involved in biological redox reactions. Typical Grxs can be divided into two major groups (monothiol and dithiol) depending on the active motif. Monothiol Grxs contain Cys-X-X-Ser as catalytic motif and dithiol Grxs share the Cys-X-X-Cys catalytic motif, similar to thioredoxins [1]. The X-X in the active site of thioredoxins can be any other amino acid but, it is restricted to PY and SY in dithiol Grxs of vertebrates [2]. In human and most of mammals, Grx1 contains CPYC as the active site and Grx2 contains CSYC [3,4]. In contrast, most of fish Grx1 consist of CSYC, and Grx2 homologs contain CPYC. In human, alteration of active site amino acids (CPYC to CSYC) has been reported to be associated with considerable variations in redox properties [5]. For example, alteration of proline to serine in mammalian Grx2 provides the ability to assemble Fe–S clusters and to accept an electron from both GSH and Thioredoxin reductase [2,5]. Moreover, it has been reported that Grx2 orthologs are capable of withstanding H_2O_2 which inhibits other Grxs [6].

The typical Grx structure is similar to thioredoxin structure and includes four β sheets surrounded by 3–5 alpha helixes [1]. Human Grx2 (HsGrx2) isoforms are lengthier than HsGrx1. They contain a similar number of active sites and beta sheets but a higher number of alpha helixes [7]. HsGrx2 isoforms can be localized either in the mitochondrion (Grx2a) or in the nucleus (Grx2b) [7]. The functions of HsGrx2 have been elucidated and it has been suggested that it is involved in several biological processes including iron-sulfur cluster formation, antiapoptotic activity, and redox homeostasis [8,9]. Moreover, the antioxidant activity and glutathionylation activity of Grxs are highly required for activating many cell signaling pathways, such as NFκB, TLR, and AKT [9–11].

In fish, Grx2 has been reported to be involved in embryogenesis, heart development, iron-sulfur cluster coordination and brain development [8,12–14]. However, existing studies on fish Grx2 mainly focus on growth and development. There are only few studies on the role of Grx2 in immune responses in aquatic organisms [15,16].

Seahorses are tiny sea creatures that have provoked curiosity due to their shape, life span, and medicinal value [17]. Almost all the seahorse

* Corresponding author. Marine Molecular Genetics Lab, Department of Marine Life Sciences, Jeju National University, 102 Jejudaehakno, Ara-Dong, Jeju, 63243, Republic of Korea.
E-mail address: jehee@jejunu.ac.kr (J. Lee).

https://doi.org/10.1016/j.fsi.2019.09.071
Received 28 June 2019; Received in revised form 26 September 2019; Accepted 30 September 2019
Available online 03 October 2019

species are recognized as endangered, and over-exploitation for medicinal purposes can be one of the threats facing seahorse populations. Therefore, the culturing of seahorses for human needs has been legalized in many countries [18]. However, seahorse farming at high densities is not very successful due to their weak immunity [19]. Based on the above facts, research on seahorse immunity will be instrumental in developing new disease control and sustainable farming strategies. Hence, this study aimed to explore the involvement of Grx2 in seahorse immunity and redox homeostasis. Therefore, a sequence that displays the highest homology to Grx2 was identified and investigated at the transcriptional and functional level.

2. Materials and methods

2.1. Identification and bioinformatic analysis of Grx2 sequence from Hippocampus abdominalis

The coding sequence (CDS) that showed the highest homology to Grx2 (HaGrx2) was identified form previously stipulated *Hippocampus abdominalis* transcriptome database [20]. The identified HaGrx2 sequence was verified and confirmed by NCBI Basic Local Search Tools (BLAST) [21]. The open reading frame (ORF) and the amino acid sequence of the protein were predicted by Unipro UGENE software [22]. Signal peptides, localization prediction, and N-linked glycosylation sites were examined by SignalP 4.0, TargetP 1.1 and NetNGlyc 1.0 online tools, respectively [23–25]. Molecular and physiochemical properties of the sequence were identified by the ExpASy Protparam tool [26]. The conserved domains and motifs were recognized by the NCBI conserved domain database (NCBI CDD) [27]. Mitochondrial processing peptidase (MPP) cleavage site was identified by MitoFates software [28], and the HeliQuest online tool was used to identify amphipathic helixes in the predicted mitochondrial target sequence of HaGrx2 [29]. The secondary structure of HaGrx2 was predicted by I-TASSER online software [30], and the three-dimensional structure was predicted by the SWISS-MODEL workbench using Protein Data Bank (PDB) template 3uiw.1 [31]. The tertiary structure of HaGrx2 protein was visualized by PyMOL 1.3 software (The PyMOL Molecular Graphics System, Version 2.0 Schrödinger, LLC). Pairwise alignment of HaGrx2 with other Grx2 orthologs was performed by MatGAT2.0 software [32], and Multiple sequence alignment of Grx2 orthologs were analyzed by CLC main workbench version 8.1.0 (https://www.qiagenbioinformatics.com/). The Phylogenetic tree was reconstructed by the neighbor-joining method (5000 bootstraps) using MEGA7 [33].

2.2. Acclimatization of big-belly seahorses, tissue sampling and immune stimulation

Healthy seahorses with an average body weight of 8 g and 12 cm of body length were purchased from Marine Ornamental Fish Breeding Center (Jeju, South Korea). Fish were acclimatized in a 300 L aquarium tank with 18 ± 2 °C temperature and 34 ± 0.6% particle salinity units (psu) for one week. Seahorses were fed with Mysis shrimp during the acclimatization period. Six healthy seashores (3 females, 3 males) were dissected, and 14 tissues were collected for tissue distribution analysis. Blood was collected by tail cutting, and peripheral blood cells were isolated by centrifugation at 3000 × *g* for 10 min at 4 °C. All tissue samples were snap frozen using liquid nitrogen and stored at −80 °C.

Seahorses were divided into five groups for immune stimulation. LPS (Sigma, USA; 1.25 μg/μL), poly I:C (Sigma, USA; 1.5 μg/μL), *Edwardsiella tarda* (*E. tarda*) (5×10^3 CFU/μL) and *Streptococcus iniae* (*S. iniae*) (1×10^5 CFU/μL) were prepared by dissolving them in 100 μL of 1 × phosphate buffer saline (PBS). Then, the individuals in each group were injected with the stimulants interperitoneally, and the control group was injected with 100 μL of 1 × PBS. After immune stimulation, blood and liver tissues were excised from five healthy seahorses from each group at 3, 6, 12, 24, 48, and 72 h post injection (p.i.). Peripheral blood cells were isolated as described in the previous paragraph. Seahorses were not fed during the challenge period. All the experiment in this study were reviewed and permitted by the Animal Care and Use Committee of Jeju National University.

2.3. RNA isolation and cDNA synthesis

Tissues were pooled to extract total RNA for tissue distribution analysis (n = 6) and temporal expression (n = 5). Total RNA was extracted by RNAiso plus (TaKaRa, Japan) and purified by RNeasy spin column (Qiagen, USA). Quality and the quantity of RNA were measured by a μDrop Plate reader (Thermo Scientific, USA) and visualized by 1.5% agarose gel electrophoresis. Isolated RNA was diluted to a final concentration of 1 μg/μL, and 1st strand cDNA was synthesized by using PrimeScript ™ II cDNA Synthesis Kit (TaKaRa, Japan). Synthesized cDNA was diluted to 40-fold in nuclease-free water and stored at −80 °C.

2.4. mRNA expression profiling by quantitative real-time PCR (qPCR) analysis

The mRNA expression profiles of both tissue distribution and temporal expression were determined by TaKaRa Thermal Cycler Dice Real Time system III (TaKaRa, Japan). All the qPCR primers were designed under the guidelines of minimum information for publication of quantitative real-time PCR experiments (MIQE) [34]. IDT PrimerQuest online Tool (https://sg.idtdna.com) was used to design the qPCR primers of HaGrx2 and seahorse 40S ribosomal protein S7 (Table 1). The seahorse 40S ribosomal protein S7 (Accession no: KP780177) was selected as the internal reference gene. The qPCR reaction was carried out in final volume of 10 μL containing 3 μL of cDNA template, 1.2 μL of nuclease-free water, 5 μL of Ex Taq ™ SYBER premix and 0.4 μL of each primer (10 pmol/μL). The qPCR thermal profile started with an initial denaturation at 95 °C for 10 min, followed by 45 cycles of 95 °C for 5 s, 58 °C for 20 s, 72 °C for 20 s. Then, a final cycle of 95 °C for 15 s, 60 °C for 30 s and 95 °C for 15 s was included for the dissociation analysis of the target. All reactions performed in triplicates.

The Livak ($2^{-\Delta\Delta CT}$) method was used to analyze the relative *HaGrx2* expression levels [35]. Ct value of lowest *HaGrx2* expressing tissue was used for the normalization in tissue-specific expression analysis. For the

Table 1
Primers used in cloning and qRT-PCR.

Primer Name	Sequence 5′–3′	Description
HaGrx2 qPCR forward	CGATGACGGCAGGAGATTAC	T_m 62 °C, 135 bp
HaGrx2 qPCR reverse	ACTAACTTGCCCTGCTGATG	T_m 62 °C, 135 bp
Seahorse 40S ribosomal S7 qPCR forward	ACTCTGGAACTGGCAGAGGAAGAC	T_m 60 °C, 187 bp
Seahorse 40S ribosomal S7 qPCR reverse	TGAAGTCATTCATGTTGGTGGCCTGTA	T_m 60 °C, 187 bp
HaGrx2 cloning forward	GAGAGAgatatcATGTTTTCTCGAGCCGGATGCTG	T_m 59.8 °C, 433 bp, pMAL-c5X, *Eco*RV
HaGrx2 cloning reverse	GAGAGAgaattcTCATTTTGCAGATTCGAATCGTCCGC	T_m 59.9 °C, 433 bp, pMAL-c5X, *Eco*RI
HaGrx2 cloning forward	GAGAGAggtaccATGTTTTCTCGAGCCGGATGCTG	T_m 59.8 °C, 433 bp, pcDNA 3.1(+), *Kpn*I
HaGrx2 cloning reverse	GAGAGAgatatcTCATTTTGCAGATTCGAATCGTCCGC	T_m 59.8 °C, 433 bp, pcDNA 3.1(+), *Eco*RV

temporal expression analysis, fold changes in *HaGrx2* expression levels at different time points were calculated using gene expression levels in PBS injected animals as controls. The data are represented as mean ± standard deviation (SD). In spatial expression analysis, statistical significance ($p < 0.05$) of the data was evaluated by the Mann Whitney *U* test using IBM SPSS 24 statistical software (IBM, USA). Differences between the expression levels in injected and un-injected animals at each time point were statistically evaluated ($p < 0.05$) using *t*-test.

2.5. Recombinant HaGrx2-pMALc5X plasmid construction

Specific HaGrx2 cloning primers with respective restriction sites (*Eco*RV and *Eco*RI) were constructed using the IDT OligoAnalyzer tool (Table 1) [36]. The CDS of the HaGrx2 was amplified using cDNA derived from brain tissue. The PCR reaction was performed by adding 2 μL of 10 pmol/μL of each primer, 5 μL of 10 × Ex Taq buffer, 4 μL of 2.5 mM dNTP, 10 μL of cDNA template, and 0.4 μL of 5U/μL Ex Taq polymerase. The PCR cycle started with an initial denaturation at 94 °C for 4 min followed by 35 cycles of 94 °C for 30 s, 55 °C for 30 s, 72 °C for 30 s and a final extension at 72 °C for 10 min. The amplified PCR product was purified by Accuprep® PCR purification kit (Bioneer co., Korea). Both PCR product and the pMAL-c5X vector (New England BioLabs Inc, USA) subjected to restriction digestion by *Eco*RV and *Eco*RI according to the manufacturer's protocol (TaKaRa, Japan). The digested PCR product and pMAL-c5X vector were purified by Accuprep® PCR purification kit and Accuprep® Gel purification kit (Bioneer Co., Korea). Then, 150 ng of digested pMAL-c5X fragments were ligated with 50 ng of digested PCR product by using 5 μL of Ligation Mighty Mix (TaKaRa, Japan) at 4 °C for 30 min. The ligated product was transformed into *E. coli* DH5α competent cells and colonies which were confirmed by colony PCR sent for the sequencing (Macrogen, Korea).

2.6. Overexpression and purification of recombinant HaGrx2

In order to express and purify the recombinant HaGrx2 protein (rHaGrx2), recombinant vectors with confirmed sequences were transformed into *E. coli* BL21 (DE3) competent cells. Cells were cultured in LB rich ampicillin medium (LB + 0.2% glucose + 100 μg/μL of ampicillin) at 37 °C with cyclic stirring at 200 rpm until 0.5 optical density at 600 nm was reached. Then cultured cells were supplemented with 1 mM isopropyl β-D-1-thiogalactopyranoside (IPTG) and further incubated at 20 °C for 8 h. Following incubation, cells were harvested by centrifugation at 4 °C, 3500 rpm for 30 min. The obtained cell pellet was resuspended in 25 mL of column buffer (20 mM Tris-HCl, 200 mM NaCl and 1 mM EDTA, pH 7.4). The fusion protein of rHaGrx2 and maltose binding protein (MBP) was purified by pMAL protein fusion and purification system (NEB, USA) based on the manufacturer's protocol. The concentration of the eluted protein was measured by Bradford's method. Protein banding pattern and purity were observed by 12% SDS-PAGE. Molecular weight of HaGrx2 and MBP was estimated as described previously [37]. The purified rHaGrx2 protein was stored at −80 °C for future use.

2.7. Cell culture and transfection of HaGrx2

PCR amplified HaGrx2 CDS was cloned into mammalian expression vector pcDNA3.1 (+) using *Kpn*I and *Eco*RV restriction sites (Table 1). Successful cloning was verified by sequencing and the plasmid was purified by QIAfilter™ Plasmid Midi Kit (Qiagen, Germany). Fathead minnow (FHM) epithelium cells were cultured in Leibovitz's L-15 medium supplemented with 10% fetal bovine serum (FBS) and 1% streptomycin and penicillin. Cells were seeded at a concentration of 3×10^5 cell/mL in 24-well plates and incubated at 25 °C for 24 h. Then the recombinant plasmid and empty pcDNA3.1 (+) vector (1 μg) were transfected into Fathead minnow (FHM) epithelium cells using X-tremeGENE™ 9 reagent following the manufacturer's protocol.

2.8. Functional assays

2.8.1. HaGrx2 deglutathionylation activity corresponds to the Human Grx1

HaGrx2 deglutathionylation was measured by a fluorescent glutaredoxin assay kit 96 well (IMCO cooperation Ltd, Sweden) according to the manufacturer's protocol. Protein samples were prepared by using 1 nM of rHaGrx2. Additionally, a control sample was prepared by replacing rHaGrx2 with 1 nM MBP. Fluorescence was measured by SYNERGY/HT™ microplate reader (Biotek, Korea). The experiment was performed in duplicates at 25 °C.

2.8.2. Oxidoreductase activity of HaGrx2

2.8.2.1. Insulin disulfide reduction activity. Antioxidant proteins such as thioredoxin and glutaredoxin can precipitate insulin by reducing disulfide bonds. The precipitate can be measured as turbidity at 650 nm. Therefore, Insulin disulfide reduction activity of rHaGrx2 was measured at 650 nm as described previously [38]. The reaction was performed in 96 well plates and consisted of a final volume of 200 μL containing 100 mM potassium phosphate buffer (pH 7.9), 2 mM bovine insulin, 2 mM EDTA and various concentrations of rHaGrx2 (0, 25, 50 μg/mL). Insulin aggregation initiated by adding 0.1 M dithiothreitol (DTT) (Sigma, USA). The insulin aggregation rate at 650 nm was recorded with 5 min intervals by Multiskan Sky microplate reader (Thermo Scientific, USA). The assay was performed in triplicates at 25 °C. The different treatments were statistically compared to control (0 μg/μL HaGrx2 + DTT) by independent *t*-test using IBM SPSS statistics 24 software.

2.8.2.2. L-dehydroascorbic (DHA) reduction assay. DHA reduction activity of rHaGrx2 was analyzed as described in Wells et al. by measuring the decrease in the absorbance at 340 nm [39]. Reaction was performed as triplicates in a final volume of 200 μL. The reaction mixture contained 2 mM EDTA, 0.2 mM NADPH, 0.1 μg/mL glutathione reductase, 1 mM GSH and different concentrations (0, 1, 2 mM) of DHA (Sigma, USA). The enzymatic reaction was initiated by adding 20 μg/mL rHaGrx2 at 25 °C. Then the absorbance measured for 2 min at 30 s intervals. Statistical significance of treatments (1 mM, 2 mM) with compared to 0 mM control at each time point were calculated by one-way ANOVA ($P > 0.05$) post hoc method using IBM SPSS statistics 24 software.

2.8.3. Cell viability assay upon H_2O_2

Un-transfected, pcDNA3.1 (+) and HaGrx2 transfected cells were incubated with different H_2O_2 concentrations (0, 200, 500 μM) for 24 h. Then, 50 μL of 4 mg/mL 3-(4,5-dimethylthiazol-2-yl)-2, 5-diphenyltetrazolium bromide (MTT) was added to each well and incubated for 2 h. The supernatant was removed by aspiration, and 150 μL of dimethyl sulfoxide (DMSO) was added to each well to dissolve the formazan crystals. Then, the absorbance was measured at 570 nm using the Multiskan Sky microplate reader (Thermo Scientific, USA). Microscopic observation of the cells in each treatment was performed by Leica DFC425C digital microscope. Study was conducted in triplicates at 25 °C.

3. Results

3.1. Bioinformatic analysis of HaGrx2

The coding sequence of identified Grx2 sequence (accession No. MK936322) was 466 bp and encoded 152 amino acids. The predicted amino acid sequence did not contain a signal peptide or N-linked glycosylation sites. The predicted molecular weight of the HaGrx2 amino acid sequence was 16.4 kDa, and theoretical p*I* was 8.88. As depicted in Fig. 1A, HaGrx2 protein consisted of a glutaredoxin domain (48–129

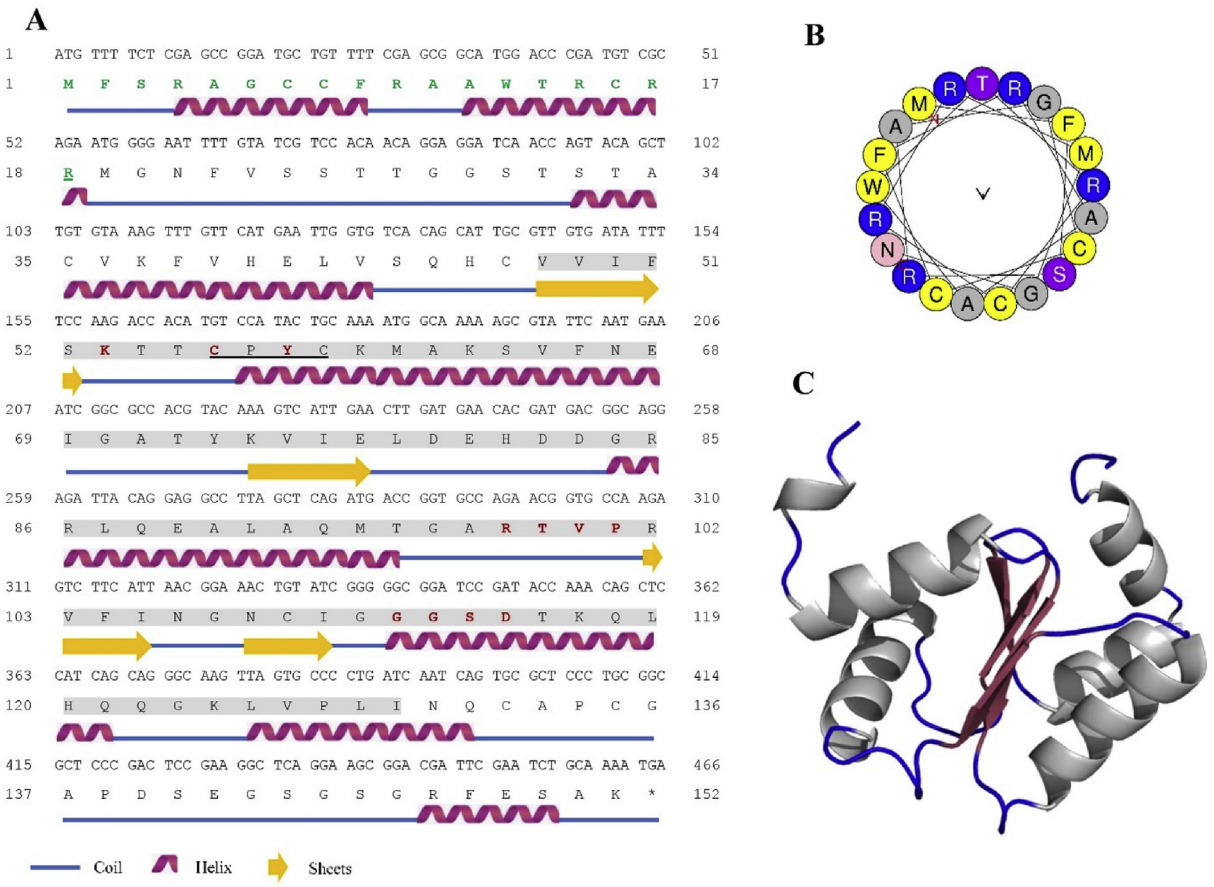

Fig. 1. (A) Nucleotide sequence, deduced amino acid sequence, and predicted secondary structure of HaGrx2. Green color letters indicate the predicted mitochondrial targeting sequence (MTS). The green color last letter (underlined) denotes the cleavage site of MTS. Predicted glutaredoxin domain highlighted with gray color and CXXC motif underlined with black color. GSH binding sites are marked with bold red color letters. (B). Predicted amphipathic helix in MTS of HaGrx2. (C) Predicted tertiary structure for HaGrx2 using 3uiw.1. A PDB template. (For interpretation of the references to color in this figure legend, the reader is referred to the Web version of this article.)

aa) and the thioredoxin/glutaredoxin CXXC active motif ^{56}CPYC^{59}. Further, it contained 11 GSH binding sites. HaGrx2 contained mitochondrial targeting peptide (MTS) and its cleavage site (Fig. 1A). In addition, MTS consisted of an amphipathic helix (Fig. 1B). According to the predicted tertiary structure, HaGrx2 has the classical glutaredoxin structure with four β sheets surrounded by five α helixes. Though the PDB template 3uiw.1. A (zebrafish Grx2) covered 81.03% of the 3D structure of HaGrx2 (Fig. 1C), it did not cover all the regions of HaGrx2 protein sequence (1-27aa and 132–151 aa). According to the predicted secondary structure (Fig. 1A), HaGrx2 contained more than six α helixes and characteristic four β sheets.

Grx2 from *Hippocampus comes,* showed the highest identity (95.4%) and similarity (96.7%) with HaGrx2 (Table 2). Grx2 of *Danio rerio* has 63.4% of identity and 75.7% of similarity with HaGrx2. According to the multiple sequence alignment, most of the amino acids are conserved in Grx2 orthologs (Fig. 2). Grx2 from *Hippocampus comes* and *Lates calcarifer* showed more conservancy with HaGrx2 compared to the rest of selected species. The CXXC motif was conserved in all selected species and was represented by CPYC in selected fish species. As showed in Fig. 2, out of 11 sites, two GSH binding sites were unique to selected fish species and the rest of the sites were conserved in all selected Grx2 orthologs. According to the phylogenetic tree (Fig. 3), selected Grx1 and Grx2 orthologs make two distinct clusters. The HaGrx2 grouped with Grx2 orthologs from fish and closely clustered with Grx2 from *Hippocampus comes.*

3.2. Spatial and temporal expression profile of HaGrx2

As shown in Fig. 4A, *HaGrx2* was ubiquitously expressed in the 14 tissues selected. The highest expression of *HaGrx2* was observed in skin and brain whereas the lowest expression was found in the liver. Temporal expression of blood *HaGrx2* upon LPS stimulation showed dynamic modulation throughout the p.i period (Fig. 4B). However, the highest *HaGrx2* upregulation was observed at 72 h p.i upon LPS, Poly I:C and *E. tarda* administration. Upon *S. iniae* infection, *HaGrx2* showed dynamic regulation and highest expression at 48 h p.i.

When considering the *HaGrx2* expression in liver, undulatory modulation upon LPS and *S. iniae* (Fig. 4C) was observed throughout the period of post injection. Regarding Poly I:C and *E. tarda,* highest *HaGrx2* expression was observed at 48 h p.i. Significant *HaGrx2* upregulation was detected at 24 h, 48 h, and 72 h p.i upon *S. iniae* challenge.

3.3. Overexpression and purification of rHaGrx2 as MBP fusion protein

According to the SDS PAGE gel image (Fig. 5), the purified rHaGrx2-MBP fusion protein appeared as a single band between 50 kDa and 70 kDa. The observed rHaGrx2-MBP fusion size (approximately 57.7 kDa) was found to be consistent with the theoretical molecular weight where MBP and rHaGrx2 account for 42.5 kDa and 16.4 kDa respectively.

Table 2
Identity and similarity percentages between Grx2 orthologs from different species.

Percentage of similarity	Name and accession number	Percentage of Identity										
		1	2	3	4	5	6	7	8	9	10	11
	1.MK_936322_*Hippocampus abdominalis*		95.4	76.2	62	63.4	71.1	41.1	41.1	41.1	38.2	43.4
	2. XP_019727358.1_ *Hippocampus comes*	96.7		76.3	62.2	64.7	72.4	42.8	41.7	41.7	36.8	43.4
	3. XP_018526333.1_ *Lates calcarifer*	82	82		76.7	60.5	69.8	41.9	41.9	42.4	33.1	40.7
	4. XP_023284517.1 _*Seriola lalandi dorsalis*	74.3	74.3	79.1		50	57.1	39.1	40.5	41.1	33.8	34.3
	5. NP_001002404.1_ *Danio rerio*	75.7	75	68.6	67.1		74.1	37.3	36.3	37.5	43.3	44.8
	6. XP_019958097.1 _*Paralichthys olivaceus*	80.3	80.3	74.4	70.7	85.1		40.6	41.2	41.8	46.6	49.2
	7. NP_001230646.1_ *Sus scrofa*	63.7	64.3	58.1	53.5	53.5	56.7		79	81.5	37.6	52.5
	8. XP_025141889.1_ *Bubalus bubalis*	63.1	61.8	58.7	56.7	55.4	56.7	85.4		96.2	38.2	50.6
	9. AAI09743.1_ *Bos taurus*	62.4	61.8	59.3	57.3	58	57.3	87.3	96.8		39.5	52.5
	10. NP_001016637.1 _*Xenopus tropicalis*	55.3	53.9	48.8	50.7	61.9	65.6	50.3	52.9	52.9		46.9
	11. XP_020646120.1 _*Pogona vitticeps*	60.5	61.2	54.1	55	67.2	69.5	64.3	65.6	65	68.8	

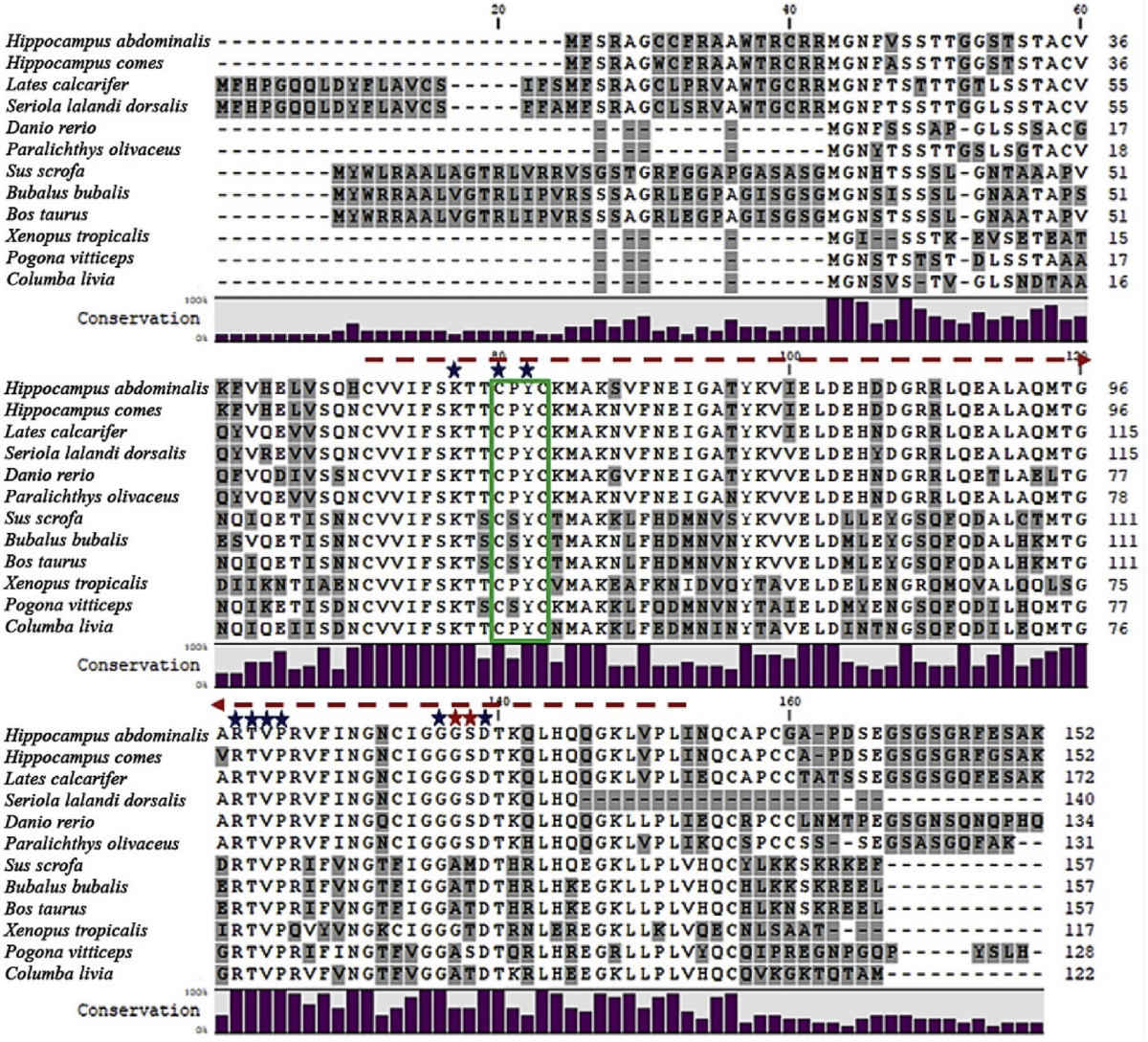

Fig. 2. Multiple-sequence alignment of Grx2 orthologs. Non-conserved residues are shaded in gray. Conservation percentage is represented as a bar plot. The conserved CXXC motif is marked with a green box, and GSH binding sites that are conserved in HaGrx2 and all other selected organisms are marked with asterisks. GSH binding sites that are conserved only in selected fish species are marked with a red color asterisk. Red arrow indicates the glutaredoxin domain Accession numbers of selected protein sequences are listed in Table 2. (For interpretation of the references to color in this figure legend, the reader is referred to the Web version of this article.)

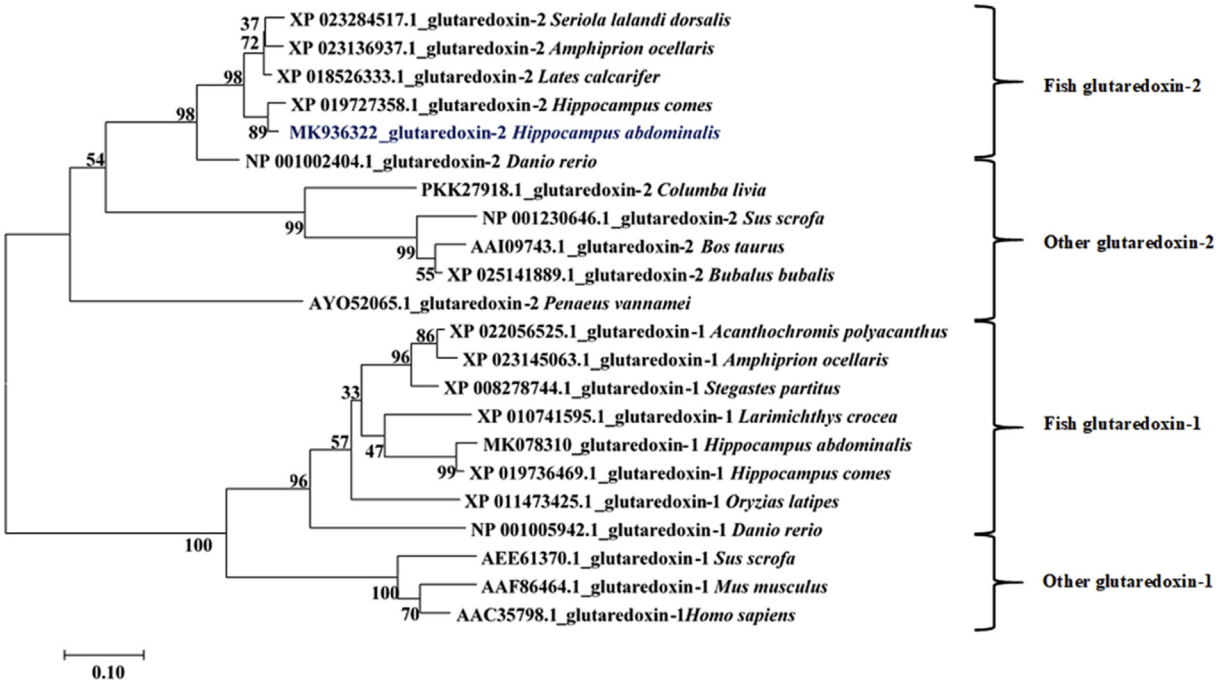

Fig. 3. Phylogenetic reconstruction of HaGrx2. Bootstrap support values corresponding to each branch are indicated.

3.4. Functional studies

3.4.1. The deglutathionylation activity of rHaGrx2 corresponded to human Grx1

According to the data obtained using the fluorescent glutaredoxin kit, 1 nM of rHaGrx2 corresponded to 0.84 nM of active HsGrx1.

3.4.2. Oxidoreductase activity of rHaGrx2

Oxidoreductase activity of HaGrx2 was assessed by the Insulin aggregation assay. As depicted in Fig. 6A, significant insulin disulfide reduction activity was observed after treating the samples with rHaGrx2 + DTT for 20 min. Higher insulin reduction activity was detected by 50 μg/mL rHaGrx2 + DTT sample than by 25 μg/mL rHaGrx2 + DTT. Except for rHaGrx2 + DTT treated samples, other treatments did not exhibit significant insulin reduction activity.

DHA reduction activity of rHaGrx2 was measured as NADPH turnover at 340 nm. According to Fig. 6B, rHaGrx2 exhibited significant DHA reduction activity that was increased with DHA concentration. MBP control and 0 mM DHA samples did not show activity at 340 nm.

3.4.3. Cytoprotective activity under oxidative stress

The cytoprotective activity of HaGrx2 was examined through cell viability upon H_2O_2 treatment. As shown in Fig. 7, HaGrx2 transfected cells showed significant cytoprotective activity compared to those of pcDNA 3.1(+) transfected cells and control cells.

4. Discussion

Grxs are abundantly expressed in most organisms and have various isoforms. When considering fish Grx2, there are four comprehensive studies on the development of zebrafish [8,12–14]. However, the importance of the redox activity of fish Grx2 for the development of immunity need to be discussed further. Therefore, in this study, we performed several functional assays related to redox activity and immunity.

3D structure of Grx2 from *Danio rerio* (3uiw.1. A) showed 81.03% sequence identity with the 3D structure of HaGrx2. However, this PDB model does not predict the full N-terminal (26 aa) and C-terminal (17aa) structure of the HaGrx2. Therefore, the secondary structure of HaGrx2 was predicted using the 3uiw.1 A PDB model, and it was found that it has additional α helixes and the same number of β sheets. However, limited data from fish species other than zebrafish make the comparison between various HaGrx2 3D structures difficult.

The deduced sequence of HaGrx2 showed the typical characteristics of Grx2 from other species. Though the length of Grx2 orthologs shows considerable variation, the glutaredoxin domain displayed more conserved features in the selected Grx2 sequences. The C-terminal and N-terminal counterparts of the Grx2 orthologs showed less conserved features. HaGrx2 exhibits more than 75% similarity and 60% identity with fish Grx2 sequences. Further, 11 GSH binding sites found in HaGrx2 are conserved among the selected fish Grx2 orthologs. Even in the phylogenetic tree, HaGrx2 tightly clustered with fish Grx2 sequences. Therefore, we can conclude that HaGrx2 shares conserved features with fish and can predict unique activities. For example, previously published studies have suggested that Grx2 is involved in critical developmental processes in fish. Zebrafish Grx2 (ZfGrx2) has been shown to regulate heart, vascular, neural and brain development of zebrafish embryo [12–14]. ZfGrx2 knockdown studies have shown that it can severely affect the development of the embryo [14].

In vertebrates, four major Grx paralogs can be found; Grx 1 and Grx2 known as dithiol glutaredoxins and Grx3 and Grx5 known as monothiol glutaredoxins [40]. According to the phylogenetic tree, HaGrx1 and HaGrx2 paralogs distinctly clade with fish Grx1 and fish Grx2, respectively. Further, they are tightly clustered with *Hippocampus comes* Grxs. It has been reported that the homology between HsGrx1 and HsGrx2 is 36% [4]. However, pairwise comparison indicated that HaGrx1 and HaGrx2 share much lower identity (24.5%) and similarity (34.6%).

HaGrx2 does not possess any signal peptide or N-linked glycosylation sites, but it has a mitochondrial targeting sequence (MTS). Many mitochondrial proteins are produced in the nucleus and translocate into mitochondria. The proteins that are produced in one subcellular organelle and translocate to another, possess target signals that allow translocation [41]. Typically, MTS is a cleavable N-terminal peptide with approximately 15–70 residues that forms an amphipathic helix [42]. HsGrx2a is a mitochondrial Grx isoform, which has MTS [7].

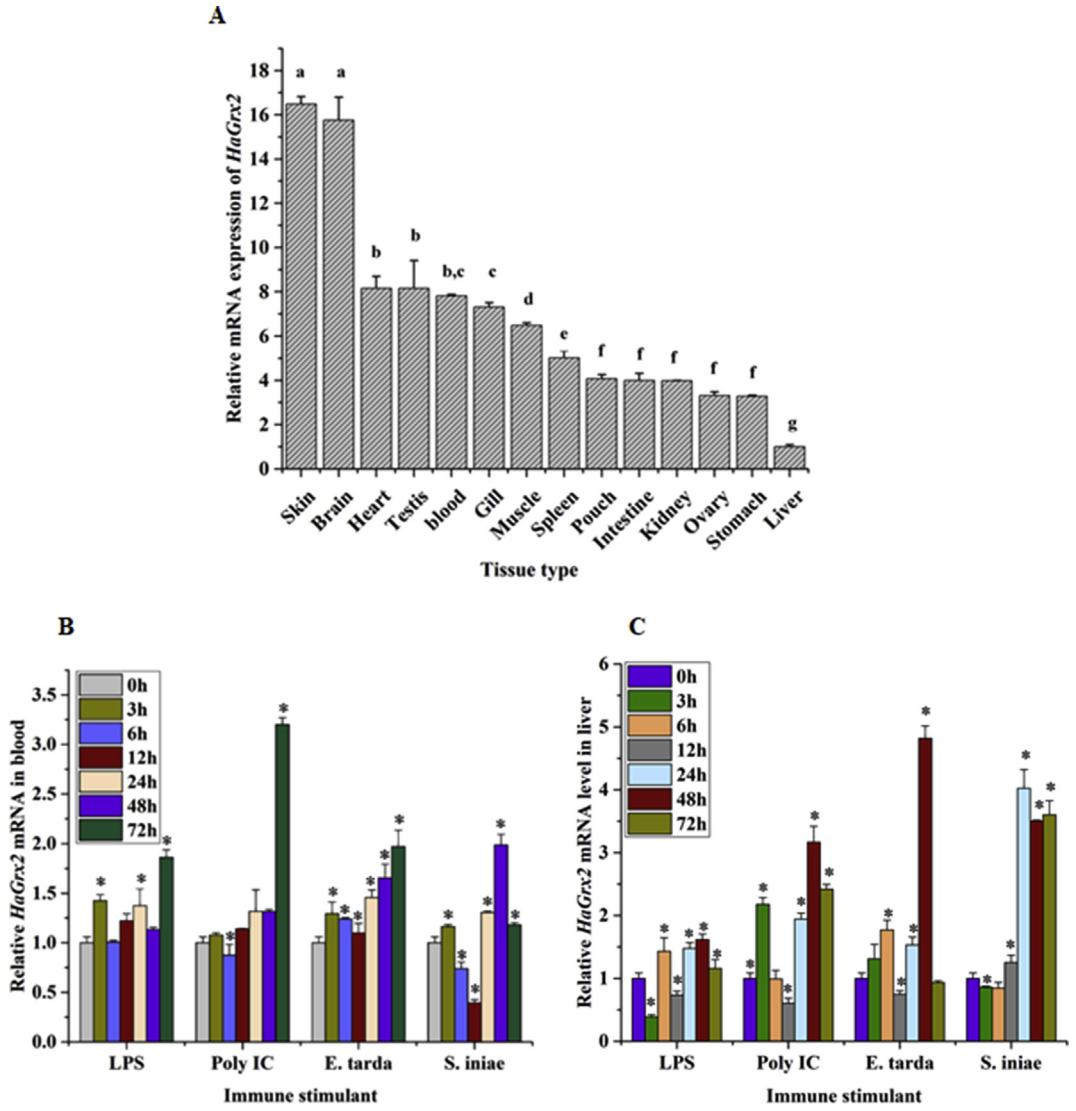

Fig. 4. (A) Tissue-specific expression of HaGrx2 under healthy conditions. Temporal expression profiles of HaGrx2 in (B) blood (C) Liver after LPS and poly I:C, *Edwardsiella tarda* and *Streptococcus iniae* challenges. The data are presented as mean values (n = 3) ± S.D. Significant differences compared to the control (0 h) are indicated with an asterisk for $p < 0.05$.

Lundberg et al. have reported that the MTS of HsGrx2a is rich in positively charged and hydrophobic amino acids and contains an MPP cleavage site. Further, the predicted secondary structure of HsGrx2a has been shown to folded into an amphipathic helix [7]. The predicted MTS for HaGrx2 contains an MPP cleavage site and presents characteristics of the amphipathic helix. Hence, bioinformatic evidences suggest that HaGrx2 is a mitochondrial protein similar to other Grx2 proteins in the vertebrates.

According to the tissue distribution analysis, highest expression was found in the skin and brain. The function of Grx2 in fish skin is not clear but it has been shown that vertebrate Grx2 is mainly involved in redox homeostasis of epithelial cell lines [6,43,44]. Knockdown of mouse Grx2 resulted in increased sensitivity to oxidative stress of lens epithelial cells [43]. Skin is the largest organ of the body that separates the internal and external environment of fish. It acts as the first line defense against many microorganisms and chemicals. Therefore, ROS produced during cell functions need to be neutralized by antioxidant proteins. Further, the skin is essential for the osmotic balance of fish and skin epithelial cells are involved in wound healing [45]. Therefore, the epithelial cells present in the skin present significant metabolic activity. Furthermore, the requirement of high energy for physiological and immune functions increases the ROS production in mitochondria. Hence, the peroxidase activity of Grx2 may be required continuously in fish skin.

The brain is also highly active in fish since brain cells make synapses with motor neurons and directly influence tail movement [46]. Seahorse has a prehensile tail that is involved in both motion and attachment to substrates. Therefore, it is expected that the brain has high energy requirements for coordinating motion. Mitochondrial complex I in brain catalyzes the first step of the mitochondrial electron transport chain [47]. Complex I contain active thiol groups that are sensitive to the redox status of the cell. The factors required for the maintenance of complex I under normal and oxidative stress conditions are not well defined. However, it has been reported that downregulation of Grx2 in the brain inhibits Complex I activity in human and mouse models [48]. Therefore, Grx2 regulate the functional integrity of the mitochondrial complex I under normal physiological conditions and high expression of *HaGrx2* transcripts in brain tissues can be explained by the above considerations.

Presence of ROS and reactive nitrogen species make proteins susceptible to irreversible oxidation by producing sulfinic and sulfonic acids [49]. Therefore, thiol-containing proteins form intermolecular bonds with GSH or other thiol-containing proteins (glutathionylation) [50]. Glutathionylated proteins have different structural and functional

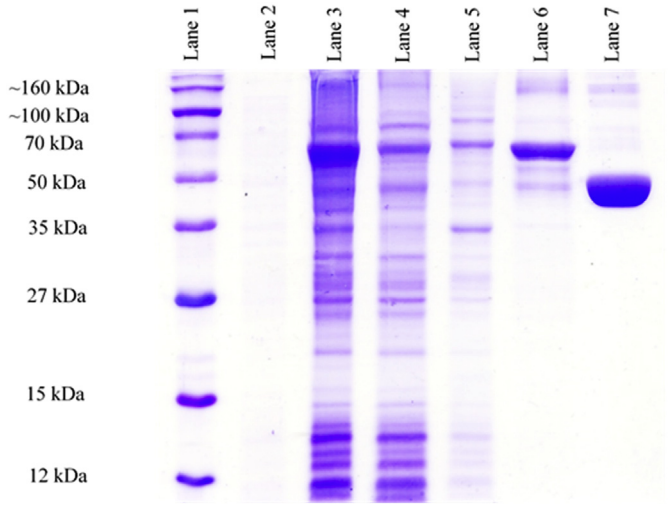

Fig. 5. SDS-PAGE analysis of overexpressed and purified HaGrx2 as an MBP-fusion protein. Lane 1: unstained protein ladder, Lane 2: crude extract of un-induced *E. coli* BL21 cells, Lane 3: crude extract of induced *E. coli* BL21 Lane 4: supernatant after sonication and centrifugation of induced *E. coli* BL21 cells, Lane 5: Pellet, Lane 6: purified HaGrx2 fusion protein, Lane 7: Purified MBP protein.

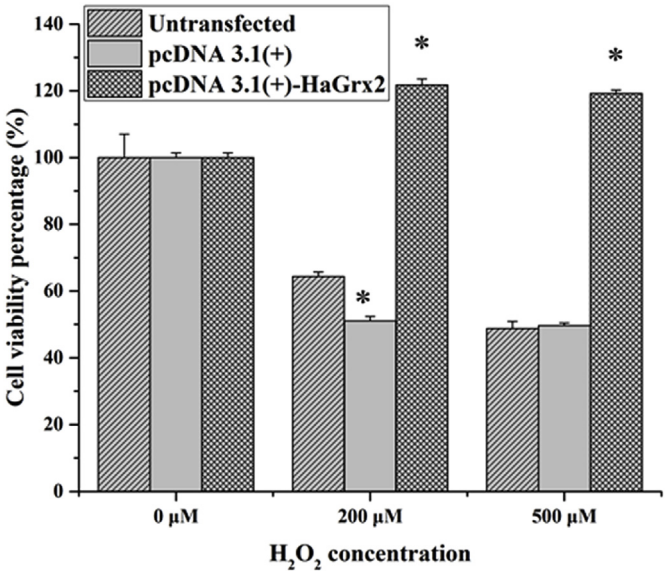

Fig. 7. Percentage viability of non-transfected, pcDNA 3.1(+) and pcDNA 3.1(+)-HaGrx2 transfected FHM cells upon H_2O_2 stress. Significant differences of treated samples compared to the control are indicated with an asterisk ($p < 0.05$).

properties than the native protein [51]. Glutathionylation acts as a protective mechanism for proteins. The functionality of the proteins is restored by deglutathionylation by glutaredoxin. This mechanism can be observed in mitochondrial complex I as it is a thiol-containing protein. Glutathionylation of complex I prevents its irreversible impairment due to H_2O_2 and reduce ROS production [6]. Mitochondrial ROS activate both antiviral and antibacterial activity as innate immune responses [52–54]. On the other hand, excessive levels of ROS can lead to impairment of several proteins and subsequently to cell apoptosis and necrosis [55]. Therefore, mitochondrial ROS production should be regulated precisely. During the high levels of oxidative stress, complex I stays in glutathionylated form and activity can be restored by Grx2 thus maintaining ROS production rate [6]. Therefore, Grx2 acts as a signaling switch in H_2O_2-mediated cell signaling and innate immune responses. According to the literature, ROS production in mitochondria is regulated by Grx2 [56].

During a bacterial infection, macrophages phagocytose bacteria. Then bacteria are lysed, and PAMPs are released that can bind to TLRs [57]. It has been reported that LPS and lipoteichoic acid (PAMP in gram-positive bacteria) can elevate mitochondrial ROS production in macrophages [58]. It has been reported that in addition to white blood cells, fish erythrocytes have also phagocytic activity [59]. Therefore, ROS produced by peripheral blood cells following PAMP and bacterial challenge are capable of activating cell signaling pathways. Hence Grx2 activity in peripheral blood cells may regulate ROS production and restore proteins that have undergone S-glutathionylation. However, the mechanism by which Grx2 precisely maintains ROS levels is not clear, because redox regulation by Grx2 is complex and depends on the type of tissue and various other factors. Based on the above facts, dynamic

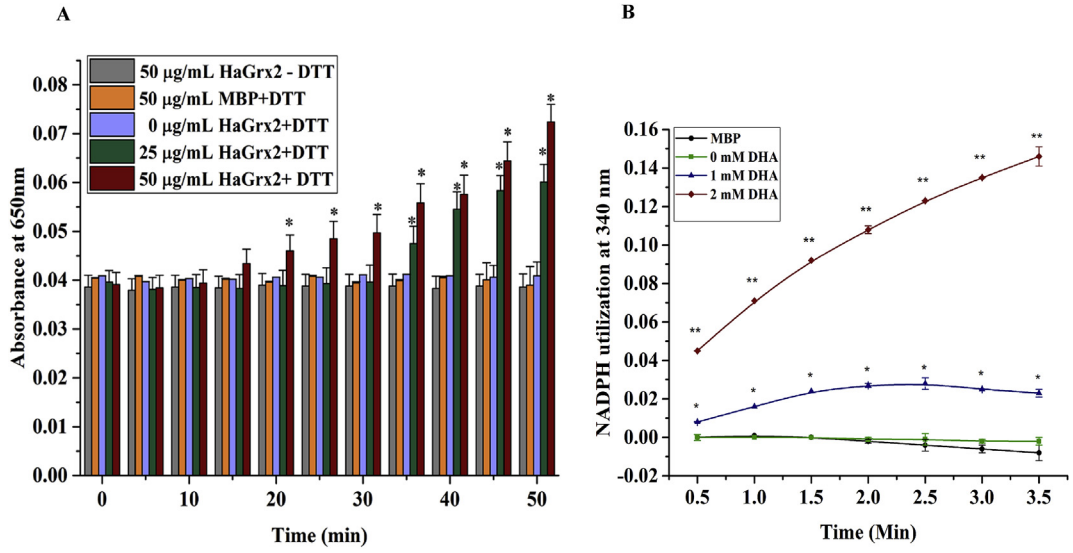

Fig. 6. (A) Insulin disulfide reduction activity of rHaGrx1 with different protein and DTT combinations. Data were obtained from triplicates and are expressed as mean values ± S.D. Significant differences ($P < 0.05$) compared to control (0 μg/mL rHaGrx1 + DTT) are indicated by *. (B) DHA reduction activity of rHaGrx2 with different DHA concentration at 25 °C. Data were obtained from triplicates. The "*" and "**" denote the significant difference ($P < 0.05$) of treatments (1 mM and 2 mM) at each time point with compared respective time points of 0 mM control.

regulation of HaGrx2 transcripts upon PAMP and bacterial stimulation in the blood is expected. Apart from bacterial PAMP, Poly I:C (viral mimic) is also identified by TLR3. TLR3-induced ROS generation leads to inflammatory responses through STAT1 activation [60]. Therefore, ROS homeostasis activity of Grx2 is required in macrophages for antiviral innate immune responses.

The same scenario was observed in the liver where Grx2 also acts as a critical regulator of ROS producing complexes. It has been reported that complex I, pyruvate dehydrogenase and 2-oxoglutarate dehydrogenase also produce ROS in liver mitochondria and are deglutathionylated by Grx2 [61]. Since Grx2 induces the activity of Complex I, pyruvate dehydrogenase and 2-oxoglutarate dehydrogenase high expression of Grx2 in the liver is expected [56]. However, Liver *HaGrx2* showed significantly higher fold expression upon exposure to live gram-positive bacteria than PAMP stimuli. It has been reported that Kupffer cells can directly bind to lipoteichoic acid in gram-positive bacteria [62]. Therefore, the liver is involved in fast elimination of pathogens from the blood. As hepatocytes are directly involved in the clearance of live pathogens, ROS-mediated antibacterial and antiviral activity may be highly required in the liver. Hence, significant Grx2 expression can be observed in both blood and liver upon immune stimulation.

As described previously, the deglutathionylation activity of Grxs is critical for cellular functions. There are many proteins that undergo deglutathionylation by Grxs. Serum albumin is an abundant plasma protein that contains ROS scavenging activity, ion binding, transport activity, and antiapoptotic activities [63]. It contains free cysteine residues that are important for the functions of the protein. During high oxidative stress, free cysteines in serum albumin are susceptible to S-glutathionylation [63]. Hence, deglutathionylation of fluorescent BSA-SSG was measured using HsGrx1 standard curve. HaGrx2 was comparable with HsGrx1 showing little lesser activity than HsGrx1. However, Lundberg et al. have suggested that HsGrx2 exhibits only 10% specific activity compared to HsGrx1 [7]. Therefore, we can predict that HaGrx2 represent higher activity than HsGrx2. The primary reason for the higher activity in HaGrx2 might be the amino acid residues present in the catalytic motif. Most mammalian Grx1 contain CPYC as a catalytic motif, and Grx2 consists of CSYC. Foloppe et al. have shown that replacement of proline residue in the Grx catalytic motif by serine can severely affect the redox properties [5]. HaGrx2 contains CPYC as the catalytic motif, which is similar to HsGrx1. Hence, HaGrx2 may contain significant deglutathionylation activity.

Mature insulin consisted of two chains named as A and B [64]. These chains are linked by inter-chain disulfide bonds and can be precipitated by reduction. Insulin precipitation assay is commonly used to measure the disulfide reduction activity of thioredoxin [65]. In this assay, DTT is used as the electron donor for the HaGrx2. It has been reported that HsGrx2 can accept electrons from sources other than GSH, such as thioredoxin reductase [2]. Though it has been accepted that Grxs have minor insulin reduction activity, HaGrx2 exhibits significant insulin reduction activity in the presence of DTT.

Ascorbic acid is a powerful antioxidant present in many organisms; however, teleost fish lack the ability to produce ascorbate due to absence of L-gulonolactone oxidase [66]. Therefore, it is essential to include vitamin C to teleost fish feed unless they develop vitamin C deficiencies and consequently impaired wound healing, reduced growth, scoliosis, low immunity, retard embryonic and larval development [66]. Further, it has been reported that, vitamin C involved in myoblast proliferation, migration, and differentiation [67]. Moreover, ascorbate acts in maintaining the redox homeostasis [68]. Therefore, other than taking vitamin C from the feed, fish should have a proper method to convert oxidized ascorbic (DHA) to ascorbate. Glutathione S-transferase omega (GSTO) converts DHA to ascorbic acid. Many studies have suggested that Grxs also contain dehydroascorbic reduction activity [39]. HaGrx2 also exhibits sound DHAR activity. Thus, we can propose that HaGrx2 regulates both redox and physiological activities in seahorse.

The antiapoptotic activity of Grx2 against H_2O_2 is widely studied in mammalian models [6,43]. According to these studies, cytoprotective activity achieved by Grx2 in various ways. Healthy epithelial cell viability decreases upon H_2O_2 stress due to BAX upregulation, BCL-2 downregulation, Caspase 3 activation, and Cytochrome C release [6]. Overexpression of Grx2 was able to sustain the BCL-2 levels even in the presence of oxidative stress. Cytochrome C release from mitochondria to cytosol is a known hallmark of apoptosis. Grx2 overexpression prevents Cytochrome C release from mitochondria [69]. Procaspase 3 is converted to Caspase 3 due to stress-induced apoptotic signals. Grx2 overexpression in epithelial cells prevents procaspase cleavage. Further, it has been shown that complex I activity is severely inhibited by H_2O_2 [47]. Grx2 is capable of preserving complex I activity directly by deglutathionylation [70]. Further, the peroxidase activity of Grx2 can also reduce H_2O_2 stress through the use of glutathione or thioredoxin reductase [44]. On the other hand, Grx2 knockdown studies have shown greater susceptibility to oxidative stress [43]. HaGrx2 also exhibits sound cytoprotective activity upon H_2O_2 treatment. Further, H_2O_2-treated HaGrx2 transfected cells demonstrated proliferative activity to some extent. This might be due to H_2O_2 scavenging and boost the metabolic activity which allows cell growth. Therefore, we can predict that Grx2 acts as an excellent antioxidant that alleviates oxidative stress-induced cell apoptosis.

According to the functional, transcriptional, and molecular investigations carried out in this study, HaGrx2 possess typical glutaredoxin structure and function. There is bioinformatic evidence that it could be a mitochondrial protein. Moreover, HaGrx2 has significant oxidoreductase and deglutathionylation activity. Spatial and temporal expression profiles revealed that it is potentially involved in physiological and immunological responses of seahorse. Most importantly, HaGrx2 exhibits cytoprotective activity against H_2O_2-induced oxidative stress. As a conclusion, the results of this study provide sufficient evidence that HaGrx2 functions in redox homeostasis as well as host immune responses.

Acknowledgments

This research was a part of the project titled ‘Fish Vaccine Research Center’, funded by the Ministry of Oceans and Fisheries, South Korea and supported by Basic Science Research Program through the National Research Foundation of Korea (NRF) funded by the Ministry of Education (2019R1A6A1A03033553).

References

[1] C.H. Lillig, C. Berndt, A. Holmgren, Glutaredoxin systems, Biochim. Biophys. Acta - Gen. Subj. 1780 (2008) 1304–1317, https://doi.org/10.1016/j.bbagen.2008.06.003.

[2] C. Johansson, C.H. Lillig, A. Holmgren, Human mitochondrial glutaredoxin reduces S-glutathionylated proteins with high affinity accepting electrons from either glutathione or thioredoxin reductase, J. Biol. Chem. 279 (2004) 7537–7543, https://doi.org/10.1074/jbc.M312719200.

[3] M.R. Fernando, H. Sumimoto, H. Nanri, S. ichiro Kawabata, S. Iwanaga, S. Minakami, Y. Fukumaki, K. Takeshige, Cloning and sequencing of the cDNA encoding human glutaredoxin, BBA - Gene Struct. Expr. 1218 (1994) 229–231, https://doi.org/10.1016/0167-4781(94)90019-1.

[4] V.N. Gladyshev, A. Liu, S.V. Novoselov, K. Krysan, Q.A. Sun, V.M. Kryukov, G.V. Kryukov, M.F. Lou, Identification and characterization of a new mammalian glutaredoxin (thioltransferase), Grx2, J. Biol. Chem. 276 (2001) 30374–30380, https://doi.org/10.1074/jbc.M100020200.

[5] N. Foloppe, L. Nilsson, The glutaredoxin -C-P-Y-C- motif: influence of peripheral residues, Structure 12 (2004) 289–300, https://doi.org/10.1016/S0969-2126(04)00021-8.

[6] H. Wu, K. Xing, M.F. Lou, Glutaredoxin 2 prevents H2O2-induced cell apoptosis by protecting complex I activity in the mitochondria, Biochim. Biophys. Acta Bioenerg. 1797 (2010) 1705–1715, https://doi.org/10.1016/j.bbabio.2010.06.003.

[7] M. Lundberg, C. Johansson, J. Chandra, M. Enoksson, G. Jacobsson, J. Ljung, M. Johansson, A. Holmgren, Cloning and expression of a novel human glutaredoxin (Grx2) with mitochondrial and nuclear isoforms, J. Biol. Chem. 276 (2001) 26269–26275, https://doi.org/10.1074/jbc.M011605200.

[8] L. Bräutigam, C. Johansson, B. Kubsch, M.A. McDonough, E. Bill, A. Holmgren, C. Berndt, An unusual mode of iron-sulfur-cluster coordination in a teleost glutaredoxin, Biochem. Biophys. Res. Commun. 436 (2013) 491–496, https://doi.org/10.

1016/j.bbrc.2013.05.132.
[9] H. Murata, Y. Ihara, H. Nakamura, J. Yodoi, K. Sumikawa, T. Kondo, Glutaredoxin exerts an antiapoptotic effect by regulating the redox state of Akt, J. Biol. Chem. 278 (2003) 50226–50233, https://doi.org/10.1074/jbc.M310171200.
[10] D. Daily, A. Vlamis-Gardikas, D. Offen, L. Mittelmani, E. Melamed, A. Holmgren, A. Barzilai, Glutaredoxin protects cerebellar granule neurons from dopamine-induced apoptosis by activating NF-κB via Ref-1, J. Biol. Chem. 276 (2001) 1335–1344, https://doi.org/10.1074/jbc.M008121200.
[11] E. Chantzoura, E. Prinarakis, D. Panagopoulos, G. Mosialos, G. Spyrou, Glutaredoxin-1 regulates TRAF6 activation and the IL-1 receptor/TLR4 signalling, Biochem. Biophys. Res. Commun. 403 (2010) 335–339, https://doi.org/10.1016/j.bbrc.2010.11.029.
[12] L. Brautigam, L.D. Schutte, J.R. Godoy, T. Prozorovski, M. Gellert, G. Hauptmann, A. Holmgren, C.H. Lillig, C. Berndt, Vertebrate-specific glutaredoxin is essential for brain development, Proc. Natl. Acad. Sci. 108 (2011) 20532–20537, https://doi.org/10.1073/pnas.1110085108.
[13] C. Berndt, G. Poschmann, K. Stühler, A. Holmgren, L. Bräutigam, Zebrafish heart development is regulated via glutaredoxin 2 dependent migration and survival of neural crest cells, Redox Biol 2 (2014) 673–678, https://doi.org/10.1016/j.redox.2014.04.012.
[14] L. Brautigam, L.D.E. Jensen, G. Poschmann, S. Nystrom, S. Bannenberg, K. Dreij, K. Lepka, T. Prozorovski, S.J. Montano, O. Aktas, P. Uhlen, K. Stuhler, Y. Cao, A. Holmgren, C. Berndt, Glutaredoxin regulates vascular development by reversible glutathionylation of sirtuin 1, Proc. Natl. Acad. Sci. 110 (2013) 20057–20062, https://doi.org/10.1073/pnas.1313753110.
[15] C. Mu, Q. Wang, Z. Yuan, Z. Zhang, C. Wang, Identification of glutaredoxin 1 and glutaredoxin 2 genes from *Venerupis philippinarum* and their responses to benzo[a] pyrene and bacterial challenge, Fish Shellfish Immunol. 32 (2012) 482–488, https://doi.org/10.1016/j.fsi.2011.12.001.
[16] P.-H. Zheng, L. Wang, A.-L. Wang, X.-X. Zhang, J.-M. Ye, D.-M. Wang, J.-F. Sun, J.-T. Li, Y.-P. Lu, J.-A. Xian, cDNA cloning and expression analysis of glutaredoxin (Grx) 2 in the Pacific white shrimp *Litopenaeus vannamei*, Fish Shellfish Immunol. 86 (2019) 662–671, https://doi.org/10.1016/j.fsi.2018.12.011.
[17] C. Woods, Aquaculture of the big-bellied seahorse Hippocampus abdominalis lesson 1827 (teleostei: syngnathidae), http://researcharchive.vuw.ac.nz/handle/10063/288, (2007).
[18] H.J. Koldewey, K.M. Martin-Smith, A global review of seahorse aquaculture, Aquaculture 302 (2010) 131–152, https://doi.org/10.1016/j.aquaculture.2009.11.010.
[19] V. Lepage, J. Young, C.J. Dutton, G. Crawshaw, J.A. Paré, M. Kummrow, D.J. Mclelland, P. Huber, K. Young, S. Russell, L. Al-Hussinee, J.S. Lumsden, Diseases of captive yellow seahorse *Hippocampus kuda* Bleeker, pot-bellied seahorse *Hippocampus abdominalis* Lesson and weedy seadragon *Phyllopteryx taeniolatus* (Lacépède), J. Fish Dis. 38 (2015) 439–450, https://doi.org/10.1111/jfd.12254.
[20] M. Oh, N. Umasuthan, D.A.S. Elvitigala, Q. Wan, E. Jo, J. Ko, G.E. Noh, S. Shin, S. Rho, J. Lee, First comparative characterization of three distinct ferritin subunits from a teleost: evidence for immune-responsive mRNA expression and iron depriving activity of seahorse (*Hippocampus abdominalis*) ferritins, Fish Shellfish Immunol. 49 (2016) 450–460, https://doi.org/10.1016/j.fsi.2015.12.039.
[21] R. Agarwala, T. Barrett, J. Beck, D.A. Benson, C. Bollin, E. Bolton, D. Bourexis, J.R. Brister, S.H. Bryant, K. Canese, C. Charowhas, K. Clark, M. Dicuccio, I. Dondoshansky, S. Federhen, M. Feolo, K. Funk, L.Y. Geer, V. Gorelenkov, M. Hoeppner, B. Holmes, M. Johnson, V. Khotomlianski, A. Kimchi, M. Kimelman, P. Kitts, W. Klimke, S. Krasnov, A. Kuznetsov, M.J. Landrum, D. Landsman, J.M. Lee, D.J. Lipman, Z. Lu, T.L. Madden, T. Madej, A. Marchler-Bauer, I. Karsch-Mizrachi, T. Murphy, R. Orris, J. Ostell, C. O'sullivan, A. Panchenko, L. Phan, D. Preuss, K.D. Pruitt, K. Rodarmer, W. Rubinstein, E. Sayers, V. Schneider, G.D. Schuler, S.T. Sherry, K. Sirotkin, K. Siyan, D. Slotta, A. Soboleva, V. Soussov, G. Starchenko, T.A. Tatusova, K. Todorov, B.W. Trawick, D. Vakatov, Y. Wang, M. Ward, W.J. Wilbur, E. Yaschenko, K. Zbicz, Database resources of the national center for biotechnology information, Nucleic Acids Res. 44 (2016) D7–D19, https://doi.org/10.1093/nar/gkv1290.
[22] K. Okonechnikov, O. Golosova, M. Fursov, A. Varlamov, Y. Vaskin, I. Efremov, O.G. German Grehov, D. Kandrov, K. Rasputin, M. Syabro, T. Tleukenov, Unipro UGENE: a unified bioinformatics toolkit, Bioinformatics 28 (2012) 1166–1167, https://doi.org/10.1093/bioinformatics/bts091.
[23] T.N. Petersen, S. Brunak, G. Von Heijne, H. Nielsen, SignalP 4.0: discriminating signal peptides from transmembrane regions, Nat. Methods 8 (2011) 785–786, https://doi.org/10.1038/nmeth.1701.
[24] O. Emanuelsson, H. Nielsen, S. Brunak, G. Von Heijne, Predicting subcellular localization of proteins based on their N-terminal amino acid sequence, J. Mol. Biol. 300 (2000) 1005–1016, https://doi.org/10.1006/jmbi.2000.3903.
[25] R. Gupta, S. Brunak, MEGA7: molecular evolutionary genetics analysis version 7.0 for bigger datasets, Biocomput 322 (1) (2002) 310–322, https://doi.org/10.1093/molbev/msw054 R. (2001).
[26] M.R. Wilkins, E. Gasteiger, A. Bairoch, J.C. Sanchez, K.L. Williams, R.D. Appel, D.F. Hochstrasser, Protein identification and analysis tools in the ExPASy server, Methods Mol. Biol. 112 (1999) 531–552, https://doi.org/10.1385/1592598900.
[27] A. Marchler-Bauer, M.K. Derbyshire, N.R. Gonzales, S. Lu, F. Chitsaz, L.Y. Geer, R.C. Geer, J. He, M. Gwadz, D.I. Hurwitz, C.J. Lanczycki, F. Lu, G.H. Marchler, J.S. Song, N. Thanki, Z. Wang, R.A. Yamashita, D. Zhang, C. Zheng, S.H. Bryant, CDD: NCBI's conserved domain database, Nucleic Acids Res. 43 (2015) D222–D226, https://doi.org/10.1093/nar/gku1221.
[28] Y. Fukasawa, J. Tsuji, S. Fu, K. Tomii, P. Horton, K. Imai, MitoFates : Improved Prediction of Mitochondrial Targeting Sequences and Their Cleavage, (2015), pp. 1113–1126, https://doi.org/10.1074/mcp.M114.043083.
[29] R. Gautier, D. Douguet, B. Antonny, G. Drin, HELIQUEST: a web server to screen sequences with specific α-helical properties, Bioinformatics 24 (2008) 2101–2102, https://doi.org/10.1093/bioinformatics/btn392.
[30] N. Khetrapal, Protein structure and function prediction using I-TASSER, Handb. Res. Hum. Cogn. Assist. Technol. Des. Access. Transdiscipl. Perspect. (2010) 96–108, https://doi.org/10.1002/0471250953.bi0508s52.
[31] M. Biasini, S. Bienert, A. Waterhouse, K. Arnold, G. Studer, T. Schmidt, F. Kiefer, T.G. Cassarino, M. Bertoni, L. Bordoli, T. Schwede, SWISS-MODEL: modelling protein tertiary and quaternary structure using evolutionary information, Nucleic Acids Res. 42 (2014) 252–258, https://doi.org/10.1093/nar/gku340.
[32] J.J. Campanella, L. Bitincka, J. Smalley, MatGAT, An application that generates similarity/identity matrices using protein or DNA sequences, BMC Bioinf. 4 (2003) 1–4, https://doi.org/10.1186/1471-2105-4-29.
[33] S. Kumar, G. Stecher, K. Tamura, MEGA7: molecular evolutionary genetics analysis version 7.0 for bigger datasets, Mol. Biol. Evol. 33 (2016) 1870–1874, https://doi.org/10.1093/molbev/msw054.
[34] S.A. Bustin, V. Benes, J.A. Garson, J. Hellemans, J. Huggett, M. Kubista, R. Mueller, T. Nolan, M.W. Pfaffl, G.L. Shipley, J. Vandesompele, C.T. Wittwer, The MIQE guidelines: minimum information for publication of quantitative real-time PCR experiments, Clin. Chem. 55 (2009) 611–622, https://doi.org/10.1373/clinchem.2008.112797.
[35] K.J. Livak, T.D. Schmittgen, Analysis of relative gene expression data using real-time quantitative PCR and the 2-ΔΔCT method, Methods 25 (2001) 402–408, https://doi.org/10.1006/meth.2001.1262.
[36] R. Owczarzy, A. V Tataurov, Y. Wu, J.A. Manthey, K.A. McQuisten, H.G. Almabrazi, K.F. Pedersen, Y. Lin, J. Garretson, N.O. McEntaggart, C.A. Sailor, R.B. Dawson, A.S. Peek, IDT SciTools: a suite for analysis and design of nucleic acid oligomers, Nucleic Acids Res. 36 (2008) W163–W169, https://doi.org/10.1093/nar/gkn198.
[37] B.-R. Laboratories, Protocol for molecular weight estimation (n.d.) 1-2, http://www.bio-rad.com/webroot/web/pdf/lsr/literature/Bulletin_6210.pdf.
[38] M. Zaffagnini, L. Michelet, V. Massot, P. Trost, S.D. Lemaire, Biochemical characterization of glutaredoxins from *Chlamydomonas reinhardtii* reveals the unique properties of a chloroplastic CGFS-type glutaredoxin, J. Biol. Chem. 283 (2008) 8868–8876, https://doi.org/10.1074/jbc.M709567200.
[39] W.W. Wells, D.P. Xu, Y. Yang, P.A. Rocque, Mammalian thioltransferase (glutaredoxin) and protein disulfide isomerase have dehydroascorbate reductase activity, J. Biol. Chem. 265 (1990) 15361–15364.
[40] E.-M. Hanschmann, J.R. Godoy, C. Berndt, C. Hudemann, C.H. Lillig, Thioredoxins, glutaredoxins, and peroxiredoxins—molecular mechanisms and health significance: from cofactors to antioxidants to redox signaling, Antioxidants Redox Signal. 19 (2013) 1539–1605, https://doi.org/10.1089/ars.2012.4599.
[41] T.D. Fox, Mitochondrial protein synthesis, import, and assembly, Genetics 192 (2012) 1203–1234, https://doi.org/10.1534/genetics.112.141267.
[42] O. Gakh, P. Cavadini, G. Isaya, Mitochondrial processing peptidases, Biochim. Biophys. Acta Mol. Cell Res. 1592 (2002) 63–77, https://doi.org/10.1016/S0167-4889(02)00265-3.
[43] H. Wu, L. Lin, F. Giblin, Y.-S. Ho, M.F. Lou, Glutaredoxin 2 knockout increases sensitivity to oxidative stress in mouse lens epithelial cells, Free Radic. Biol. Med. 51 (2011) 2108–2117, https://doi.org/10.1016/j.freeradbiomed.2011.09.011.
[44] M.R. Fernando, J.M. Lechner, S. Löfgren, V.N. Gladyshev, M.F. Lou, Mitochondrial thioltransferase (glutaredoxin 2) has GSH-dependent and thioredoxin reductase-dependent peroxidase activities in vitro and in lens epithelial cells, FASEB J. 20 (2006) 2645–2647, https://doi.org/10.1096/fj.06-5919fje.
[45] M. Ángeles Esteban, R. Cerezuela, Fish Mucosal Immunity: Skin BT - Mucosal Health in Aquaculture, Elsevier Inc., 2015, https://doi.org/10.1016/B978-0-12-417186-2/00004-2.
[46] Division of labour in the fish brain | Max-Planck-Gesellschaft (n.d.), https://www.mpg.de/division-of-labour-in-the-fish-brain (accessed April 16, 2019).
[47] G. Lenaz, R. Fato, M.L. Genova, C. Bergamini, C. Bianchi, A. Biondi, Mitochondrial complex I: structural and functional aspects, Biochim. Biophys. Acta Bioenerg. 1757 (2006) 1406–1420, https://doi.org/10.1016/j.bbabio.2006.05.007.
[48] S. Karunakaran, U. Saeed, S. Ramakrishnan, R.C. Koumar, V. Ravindranath, Constitutive expression and functional characterization of mitochondrial glutaredoxin (Grx2) in mouse and human brain, Brain Res. 1185 (2007) 8–17, https://doi.org/10.1016/j.brainres.2007.09.019.
[49] M. Lo Conte, K.S. Carroll, The redox biochemistry of protein sulfenylation and sulfinylation, J. Biol. Chem. 288 (2013) 26480–26488, https://doi.org/10.1074/jbc.R113.467738.
[50] C.L. Grek, J. Zhang, Y. Manevich, D.M. Townsend, K.D. Tew, Causes and consequences of cysteine s-glutathionylation, J. Biol. Chem. 288 (2013) 26497–26504, https://doi.org/10.1074/jbc.R113.461368.
[51] E. Belcastro, C. Gaucher, A. Corti, P. Leroy, I. Lartaud, A. Pompella, Regulation of protein function by S-nitrosation and S-glutathionylation: processes and targets in cardiovascular pathophysiology, Biol. Chem. 398 (2017) 1267–1293, https://doi.org/10.1515/hsz-2017-0150.
[52] M. Pourcelot, D. Arnoult, Mitochondrial dynamics and the innate antiviral immune response, FEBS J. 281 (2014) 3791–3802, https://doi.org/10.1111/febs.12940.
[53] Y. Chen, Z. Zhou, W. Min, Mitochondria, oxidative stress and innate immunity, Front. Physiol. 9 (2018) 1–10, https://doi.org/10.3389/fphys.2018.01487.
[54] P.D. Ray, B.-W. Huang, Y. Tsuji, Reactive oxygen species (ROS) homeostasis and redox regulation in cellular signaling, Cell. Signal. 24 (2012) 981–990, https://doi.org/10.1016/j.cellsig.2012.01.008.Reactive.
[55] S. Di Meo, T.T. Reed, P. Venditti, V.M. Victor, Harmful and beneficial role of ROS 2017, Oxid. Med. Cell. Longev. 2018 (2018) 1–2, https://doi.org/10.1155/2018/5943635.
[56] J. Chalker, D. Gardiner, N. Kuksal, R.J. Mailloux, Characterization of the impact of

glutaredoxin-2 (GRX2) deficiency on superoxide/hydrogen peroxide release from cardiac and liver mitochondria, Redox Biol 15 (2018) 216–227, https://doi.org/10.1016/j.redox.2017.12.006.
[57] S.H.E. Kaufmann, A. Dorhoi, Molecular determinants in phagocyte-bacteria interactions, Immunity 44 (2016) 476–491, https://doi.org/10.1016/j.immuni.2016.02.014.
[58] A.P. West, I.E. Brodsky, C. Rahner, D.K. Woo, H. Erdjument-Bromage, P. Tempst, M.C. Walsh, Y. Choi, G.S. Shadel, S. Ghosh, TLR signalling augments macrophage bactericidal activity through mitochondrial ROS, Nature 472 (2011) 476–480, https://doi.org/10.1038/nature09973.
[59] L. Passantino, A. Cianciotta, E. Jirillo, M. Altamura, G.F. Passantino, A. Tafaro, R. Patruno, Fish immunology. I. Binding and engulfment of *Candida albicans* by erythrocytes of rainbow trout (*Salmo gairdneri* richardson), Immunopharmacol. Immunotoxicol. 24 (2002) 665–678, https://doi.org/10.1081/iph-120016050.
[60] C.-S. Yang, J.-J. Kim, S.J. Lee, J.H. Hwang, C.-H. Lee, M.-S. Lee, E.-K. Jo, TLR3-Triggered reactive oxygen species contribute to inflammatory responses by activating signal transducer and activator of transcription-1, J. Immunol. 190 (2013) 6368–6377, https://doi.org/10.4049/jimmunol.1202574.
[61] J.M. May, S. Mendiratta, K.E. Hill, R.F. Burk, Reduction of dehydroascorbate to ascorbate by the selenoenzyme thioredoxin reductase, J. Biol. Chem. 272 (1997) 22607–22610, https://doi.org/10.1074/jbc.272.36.22607.
[62] C. Llorente, B. Schnabl, Fast-track clearance of bacteria from the liver, Cell Host Microbe 20 (2016) 1–2, https://doi.org/10.1016/j.chom.2016.06.012.
[63] A.J. Lepedda, A. Zinellu, G. Nieddu, P. De Muro, C. Carru, R. Spirito, A. Guarino, F. Piredda, M. Formato, Human serum albumin Cys 34 oxidative modifications following infiltration in the carotid atherosclerotic plaque, Oxid. Med. Cell. Longev. 2014 (2014) 1–7, https://doi.org/10.1155/2014/690953.
[64] M. Weiss, D.F. Steiner, L.H. Philipson, Insulin Biosynthesis, Secretion, Structure, and Structure-Activity Relationships, MDText.com, Inc., 2000 doi:25905258.
[65] A. Holmgren, Thioredoxin catalyzes the reduction of insulin disulfides by dithiothreitol and dihydrolipoamide, J. Biol. Chem. 254 (1979) 9627–9632 doi:10.10.79.
[66] B. Ching, S.F. Chew, Y.K. Ip, Ascorbate synthesis in fishes: a review, IUBMB Life 67 (2015) 69–76, https://doi.org/10.1002/iub.1360.
[67] B.O.S. Duran, G.A. Góes, B.T.T. Zanella, P.P. Freire, J.S. Valente, R.A.S. Salomão, A. Fernandes, E.A. Mareco, R.F. Carvalho, M. Dal-Pai-Silva, Ascorbic acid stimulates the in vitro myoblast proliferation and migration of pacu (*Piaractus mesopotamicus*), Sci. Rep. 9 (2019) 1–12, https://doi.org/10.1038/s41598-019-38536-4.
[68] J.X. Wilson, J.X. Wilson, The physiological role of dehydroascorbic acid, FEBS Lett. 527 (2002) 5–9, https://doi.org/10.1016/S0014-5793(02)03167-8.
[69] M. Enoksson, A.P. Fernandes, S. Prast, C.H. Lillig, A. Holmgren, S. Orrenius, Overexpression of glutaredoxin 2 attenuates apoptosis by preventing cytochrome c release, Biochem. Biophys. Res. Commun. 327 (2005) 774–779, https://doi.org/10.1016/j.bbrc.2004.12.067.
[70] R.S. Kenchappa, V. Ravindranath, Glutaredoxin is essential for maintenance of brain mitochondrial complex I: studies with MPTP, FASEB J. 17 (2003) 717–719, https://doi.org/10.1096/fj.-02.